EurJIC
European Journal of Inorganic Chemistry

Research Article
doi.org/10.1002/ejic.202400344

Chemistry Europe
European Chemical Societies Publishing

www.eurjic.org

Organotellurium(II) and -(IV) Compounds with Picolinoylbis(thioureas): From Simple 1:1 Adducts to Multimetallic Aggregates

Sailer S. dos Santos,[a] Vania D. Schwade,[a] Ernesto Schulz Lang,[a] Chien Thang Pham,[b] Maximilian Roca Jungfer,[c] Ulrich Abram,*[d] and Hung Huy Nguyen*[b]

Reactions of 2,6-dipicolinoylbis(*N,N*-diethylthiourea) (H_2L^{Et}) with common tellurium(IV) starting materials such as $PhTeBr_3$ or $TeBr_4$ yield various tellurium(IV) and tellurium(II) compounds depending on the conditions applied. Equimolar amounts of H_2L^{Et} and $PhTeBr_3$ give the 1:1 complex $[PhTe^{IV}Br_3(H_2L^{Et})]$, while with an excess of H_2L^{Et}, the tellurium compound is partially reduced and a $\{PhTe^{II}\}^+$ building block coordinates to both sulfur atoms of H_2L^{Et} under the formation of the ion pair $[PhTe^{II}(H_2L^{Et})][PhTe^{IV}Br_4]$. Similar reactions between H_2L^{Et} and $TeBr_4$ give the neutral monomer $[Te^{II}Br_2(H_2L^{Et})]$ or the coordination polymer $[Te^{II}Br_2(H_2L^{Et})]_\infty$. The latter compound is also formed with the assistance of Pb^{2+} ions. While the lead ions do not appear in the isolated product, similar reactions with transition metal ions such as Ni^{2+}, Mn^{2+}, or Co^{2+} result in the formation of heterobimetallic complexes, in which Te(II) building blocks are directed to the sulfur atoms of the deprotonated ligand $\{H_2L^{Et}{}_2\text{-}S,S\}^{2-}$, while the transition metal ions occupy central coordination positions between two of the organic ligands using the pyridine nitrogen atom, carbonyl oxygen atom(s) and/or the nitrogen atoms of the thiourea units.

Introduction

The coordination chemistry of tellurium with organic ligands is less explored compared to that of other main group metals. Studies on Te(II) and Te(IV) complexes are mainly directed to adducts with neutral ligands.[1–4] According to Pearson's concept of 'hard' and 'soft' acids and bases,[5] both Te(IV) and Te(II) ions can be classified as 'soft' acids. Thus, the complex formation with oxygen or nitrogen-donor ligands is not preferred and the adducts are frequently unstable.[6–8] By contrast, Te(II) and Te(IV) complexes with various sulfur-containing ligands are well-known, including a wide range of substituted thioureas and thiones,[9–15] as well as some phosphine sulfide- and some thioether-based ligands.[7,16] Even though almost 150 thiourea-type complexes of tellurium have been studied by X-ray diffraction,[17] there are only two examples of *S,O* chelates.[18,19] This also includes the large class of aroyl(*N,N*-dialkylthiourea) ligands (HR_2btu, Scheme 1), which form stable chelates with a huge variety of metal ions,[20–24] and act as monodentate ligands only in exceptional cases (e.g. with strongly thiophilic metal ions such as Ag^+, Hg^{2+} or Cu^+).[25–33] Only in one very early report, the ligation of aroyl(*N*-alkylthioureas) to tellurium in the form of $[TeCl_4(S\text{-}HR_2btu)_2]$ complexes was concluded from elemental analyses and spectroscopical data.[34]

2,6-Dipicolinoylbis(*N,N*-dialkylthioureas) (H_2L^R, Scheme 1) possess two chelating aroyl(*N,N*-dialkylthiourea) units and a central pyridine-2,6-dicarboxamide pincer moiety. Interestingly, there are hitherto only a few examples of a complex formation between H_2L^R with metal ions of only one element. 'Soft' metal ions such as Ag^+, Cu^+, or In^{3+} prefer the coordination via the sulfur atoms or the *S,O* chelating units of H_2L^R ligands, while 'harder' ions such as $(UO_2)^{2+}$ also use the central *O,N,O* coordination site.[35–40] A remarkable binding situation is found in the binuclear nickel complex $[Ni_2(L^{Et})_2(MeOH)_2]$, which contains two six-coordinate Ni^{2+} ions in completely different coordination environments.[41] One-pot reactions between H_2L^R ligands and a mixture of 'hard' metal ions such as alkali, alkaline earth metal or lanthanides ions and 'intermediate soft' metal ions such as Ni^{2+}, Co^{2+}, Mn^{2+} etc., however, give more regular

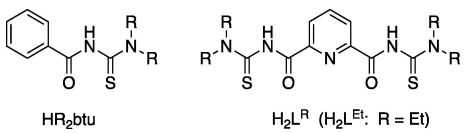

HR_2btu H_2L^R (H_2L^{Et}: R = Et)

Scheme 1. Aroylthioureas relevant for the present paper.

[a] *S. S. dos Santos, V. D. Schwade, E. S. Lang*
Laboratório de Materiais Inorgânicos, Departamento de Química, Universidade Federal de Santa Maria, 97105-900 Santa Maria, RS, Brazil

[b] *C. T. Pham, H. H. Nguyen*
Department Department of Inorganic Chemistry, VNU University of Science, 19 Le Thanh Tong, 110403 Hanoi, Vietnam
E-mail: nguyenhunghuy@hus.edu.vn

[c] *M. Roca Jungfer*
Ruprecht-Karls Universität Heidelberg, Im Neuenheimer Feld 271, D-69120 Heidelberg, Germany

[d] *U. Abram*
Institute of Chemistry and Biochemistry, Freie Universität Berlin, Fabeckstr. 34/36, D-14195 Berlin, Germany
E-mail: ulrich.abram@fu-berlin.de

Supporting information for this article is available on the WWW under https://doi.org/10.1002/ejic.202400344

Research Article
doi.org/10.1002/ejic.202400344

arrangements with the peripheral *S,O* chelating units coordinating to the 'softer' metal ions, while the 'hard' metal ions are accommodated in the central *O,N,O* cavities (Scheme 2). The products show remarkable optical and magnetic properties depending on the individual metal ions applied.[41] A special type of compounds is formed when Au^{+} ions are used in combination with lanthanides, other M^{3+} ions or alkaline earth ions. They form macrocyclic $\{Au_3(L^R)_3\}^{3-}$ or $\{Au_4(L^R)_4\}^{4-}$ ring systems, which accommodate Ln^{3+} or each two alkaline earth cations in their central cavities (Scheme 2).[42,43] Recently, such compounds with the radioactive isotopes ^{198}Au, ^{177}Lu and/or ^{68}Ga even found consideration as potential components for (radio)pharmaceutical preparations.[44]

The present report describes the coordination chemistry of tellurium(IV) and tellurium(II) building blocks with the H_2L^{Et} ligand and the formation of mixed-metal complexes with transition metal ions.

Results and Discussion

Reactions of H_2L^{Et} with $PhTeBr_3$

$PhTeBr_3$ readily reacts with H_2L^{Et} in MeOH without the addition of any supporting base under the formation of the adduct $[PhTeBr_3(H_2L^{Et})]$ (**1**). The product is only moderately soluble in MeOH and quickly precipitates from the reaction mixture at ambient temperature. The microcrystalline yellow solid was filtered off and recrystallized from CH_2Cl_2/MeOH giving yellow plates suitable for X-ray diffraction. A few orange-red crystals of a second product, $[PhTe(H_2L^{Et})][PhTeBr_4]$ (**2**), could be isolated from the remaining mother solution upon standing for some days at room temperature (Scheme 3). Compound **2** is formed by partial reduction of the Te(IV) starting material with H_2L^{Et} as reductant. The addition of an excess of 2,6-dipicolinoylbis(*N,N*-diethylthiourea) increases the yield of the Te(II) product, but the formation of the oxidized ligand hinders the isolation of compound **2** of reasonable purity. The formation of **2** is also observed when the adduct complex **1** is treated with H_2L^{Et} at elevated temperature.

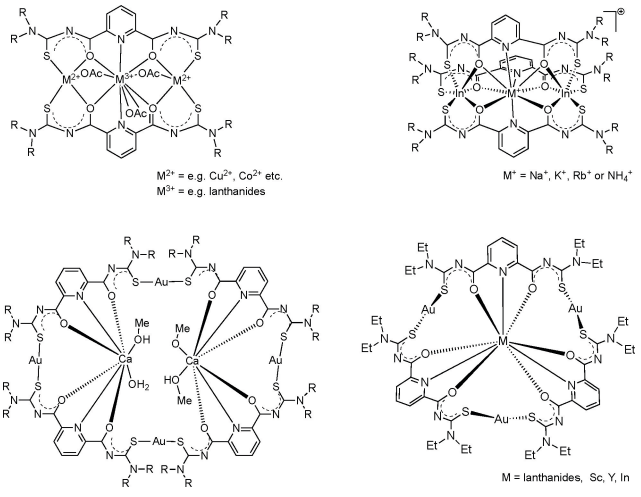

Scheme 2. Bimetallic complexes formed with 2,6-dipicolinoylbis(*N,N*-dialkylthiourea) ligands.

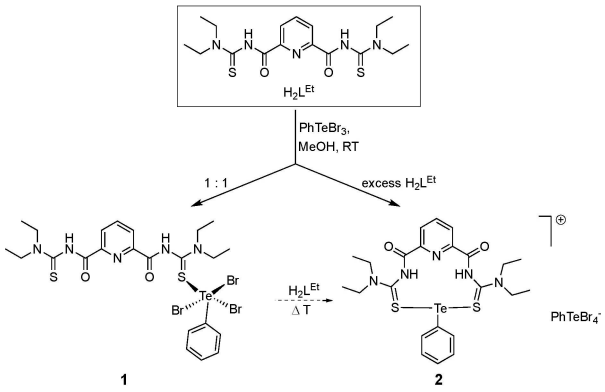

Scheme 3. Reactions of H_2L^{Et} with $PhTeBr_3$.

The coordination of the H_2L^{Et} ligand in the two tellurium complexes **1** and **2** in its non-deprotonated form is confirmed by the detection of ν_{NH} stretches in the IR spectra of the products at 3140 (**1**) and 3189 cm^{-1} (**2**). The vibrations of C=O groups appear as strong and sharp absorptions at 1709 cm^{-1} and 1680 cm^{-1} for compound **1** and at 1725 cm^{-1} for complex **2**. These wavenumber values are much higher than those observed in the IR spectra of complexes with *S,O*-chelating benzoylthioureato ligands, where they appear around 1550 cm^{-1},[23,24] but in the same ranges of $\nu_{C=O}$ stretches observed in monodentate, neutral, *S*-bonded benzoylthiourea complexes.[45,46]

The information derived from the IR spectra of **1** and **2** is consistent with the NMR data obtained for compound **1**. A broad singlet at 10.25 ppm in the ^{1}H NMR spectrum of **1** verifies the presence of two NH protons. Other chemical shifts belonging to coordinated H_2L^{Et} in **1** are all very similar to those found in the ^{1}H and ^{13}C NMR spectra of the uncoordinated ligand.[35,37–39] They clearly confirm the neutral *S*-bonded coordination fashion of H_2L^{Et}. The hindered rotation of the NEt_2 moiety around the C(S)-NEt_2 bond causes two separated signal sets of *N,N*-diethylthiourea groups in the ^{1}H NMR spectra, including two broadened quartets at 4.05 ppm and 3.76 ppm, and two overlapped triplets at 1.40 ppm. The hindered rotation in such aroylthioureato ligands is common and associated with a rotational barrier in the magnitude of approximately 60 kJ/mol.[48] The proton resonances of the pyridine ring are also slightly broadened and clearly show the coupling pattern of an AB_2 system. The ^{125}Te NMR spectrum of **1** in $CDCl_3$ presents only one signal at 1204.3 ppm. This finding is within the common range of Te(IV) compounds.[47,49–51] Further support for the structure of **1** is given by the ESI(+) MS spectrum of the product. It reveals a moderately intense signal at m/z = 600.0755, which can be assigned to the cationic fragment $\{M - 2HBr - Br\}^+$. The low solubility of compound **2** prevents the recording of NMR and mass spectra of sufficient quality.

Single-crystal X-ray diffraction studies on **1** and **2** confirm the conclusions drawn from the spectroscopic data for both

Research Article
doi.org/10.1002/ejic.202400344

compounds. The molecular structure of **1** and the structure of the complex cation of **2** are depicted in Figure 1. Selected bond lengths and angles are listed in Table 1. The coordination environment of the tellurium(IV) atom in compound **1** is a tetragonal pyramid with a monodentate, *S*-bonded H_2L^{Et} ligand. The four positions of the square plane are occupied by three bromido ligands and one of the *S*-donor atoms of H_2L^{Et}, whereas the apical position is completed by the phenyl ring.

The protonation of N9 and N19 is experimentally confirmed by the detection of electron density peaks in the final Fourier map, which have been assigned to the corresponding hydrogen atoms and refined. These H atoms establish weak hydrogen bonds to the pyridine nitrogen atom. Expectedly, two different C–S bonds are found in compound **1**. While the C20–S2 bond length of 1.671(5) Å is in the range of the C=S bonds in uncoordinated H_2L^{Et},[37] the C10–S1 bond distance of 1.721(5) Å is slightly longer, but in the same range as in other complexes with monodentate, *S*-bonded aroylthioureas.[26,45] In compound **1**, the Te–S distance of 2.689(1) Å is actually longer than the Te–Br bond lengths (see Table S2.2 of the Supporting Information), indicating a relatively weak interaction and is consistent with the monodentate neutral, *S*-bonded coordination mode of H_2L^{Et}.

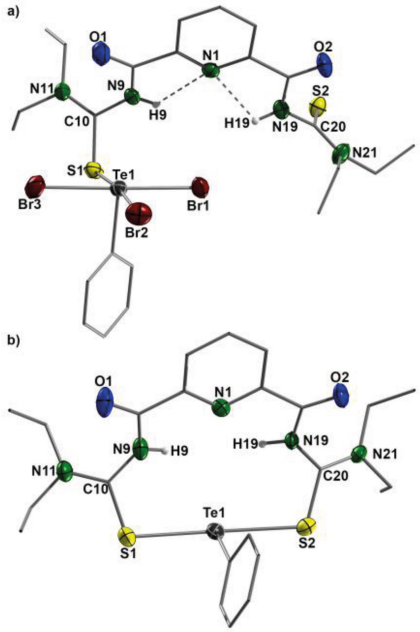

Figure 1. a) Molecular structure of compound **1** and b) structure of the complex cation of **2**. Hydrogen atoms (except of the amide H atoms) are omitted for clarity. Thermal ellipsoids are shown with 50 per cent probability.

Table 1. Selected bond lengths/Å and angles/° in compounds **1** and **2**.

	1	2		1	2
Te1–S1	2.689(1)	2.673(2)	Te1–S1–C10	98.3(2)	106.3(3)
Te1–S2	–	2.694(2)	Te1–S2–C20	–	106.0(2)
S1–C10	1.721(5)	1.706(9)	S1–Te1–S2	–	176.76(8)
S2–C20	1.671(5)	1732(8)			

The asymmetry observed in the solid-state structure of compound **1** is not reflected by its ^{1}H and ^{13}C NMR spectra, suggesting a dynamic equilibrium in solution, which is fast at the NMR time scale. This can be rationalized by the significantly larger size of H_2L compared to typical monodentate neutral thioureas, as well as the weak coordination bond between Te and H_2L^{Et}.

The complex cation of **2** contains the tellurium atom in a T-shaped coordination environment formed by the phenyl ligand and the two S atoms of H_2L^{Et} (Figure 1b). The dipicolinoylbis(*N,N*-diethylthiourea) remains protonated and forms a 12-membered ring with an almost linear S1–Te2–S2 unit. Such a coordination mode is unprecedented for H_2L^{R} ligand systems. The C(phenyl)–Te1–S1/S2 bond angles are close to 90.0°, which reflects only weak repulsive effects of the lone pairs of the Te(II) ion, while the widening of the Te–S–C angles in **2** compared to the value in **1** is a hint for some steric strain inside the 12-membered ring. Albeit the lone pair of the pyridine N atom is directed towards Te1, the tellurium-nitrogen distance of 3.964(8) Å is too long to conclude any bonding interactions between the two atoms.

The bifunctional thiourea H_2L^{Et} acts as a reductant for the $PhTeBr_3$ starting material and causes the formation of the cationic tellurium(II) complex of compound **2**. This is proven by the detection of the corresponding disulfide in the reaction mixture (details about its structure and its abilities to act also as a ligand are given vide infra). Compound **2** is only formed as a minor side product in the reaction mixture containing equivalent amounts of $PhTeBr_3$ and H_2L^{Et} at room temperature, while an excess of the thiourea increases the amount of the tellurium(II) complex. The same is observed when solutions of **1** are kept at elevated temperatures for a longer time, whereas the compound is stable at room temperature as has been proven by NMR experiments. Partially oxidized H_2L^{Et} are also found as ligands of some mixed-metal complexes (vide infra). Although a detailed mechanism cannot be derived from these data concerning the relatively long accumulation times for ^{125}Te NMR spectra of reasonable quality, the experiments suggest that the oxidation of H_2L^{Et} occurs in uncoordinated as well as in (mono)coordinated form and is slow compared to the formation of compound **1**.

Reactions of H_2L^{Et} with $TeBr_4$

$TeBr_4$ is a stronger oxidant than $TePhBr_3$.[1,2] Thus, the treatment of $TeBr_4$ with an equivalent amount of H_2L^{Et} in MeOH results in a quick color change from yellow to orange-red. The ^{125}Te NMR spectrum of the reaction mixture reveals the absence of the resonance of the starting material $TeBr_4$ at 1282 ppm and the presence of at least two signals in the region of 720 ppm, which is characteristic for Te(II) compounds.[47,49–51] Consequently, a product similar to compound **1** is not stable and undergoes a rapid reduction under formation of Te(II) products. An orange-red solid of the composition $[TeBr_2(H_2L^{Et})]$ (**3**) was finally isolated, when $TeBr_4$ and H_2L^{Et} were used in a ratio of 1:3 (Scheme 4). Under such conditions, compound **3** precipitates in

Research Article
doi.org/10.1002/ejic.202400344

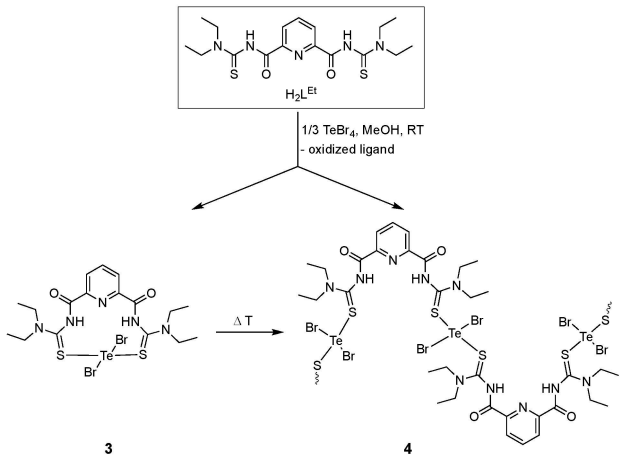

Scheme 4. Reactions of H_2L^{Et} with $TeBr_4$.

yields up to 90 %. Interestingly, some single crystals of a second product, a polymeric complex with the same chemical composition, $[TeBr_2(H_2L^{Et})]_\infty$ (**4**), could be obtained from the remaining mother solution after standing for several days in a refrigerator. Despite the very slow conversion of the monomeric complex **3** to the polymeric complex **4** at room temperature, this process is accelerated at higher temperatures. Heating of $CHCl_3$/EtOH solutions of compound **3** for several hours forms **4** as a fine powder, which precipitates from the solution and is almost insoluble in common solvents. The formation of polymer **4** has also been observed during an attempted reaction between H_2L^{Et}, $TeBr_4$ and lead(II) acetate.

The IR spectra of complexes **3** and **4** exhibit medium ν_{N-H} stretches in the region above 3100 cm^{-1}. This aspect indicates that the organic ligands are not deprotonated in these products. Their $\nu_{C=O}$ stretches are found at 1715 (**3**) and 1711 cm^{-1} (**4**), which corresponds to a blue shift relative to the position in the uncoordinated H_2L^{Et} (two bands at 1686 and 1672 cm^{-1}, where the carbonyl groups are involved in intermolecular hydrogen bonds).[37] This finding strongly supports the existence of non-coordinated C=O groups in **3** and **4**, which do not form hydrogen bonds.

While the polymeric compound **4** is practically insoluble and, thus, gives no NMR or mass spectra of sufficient quality, the monomeric complex **3** is readily soluble in acetone and chlorinated organic solvents such as $CHCl_3$ or CH_2Cl_2. A broad resonance at 10.48 ppm in the ^1H NMR spectrum of **3** is consistent with the observation of NH stretches in its IR spectrum and confirms a neutral coordination model of the ligand. A doublet at 8.41 ppm and a triplet at 8.31 ppm can be assigned to pyridine protons and reflect a symmetric bonding situation of the organic ligand. A hindered rotation of the NEt_2 moiety around C(S)–NEt_2 can also be derived from the proton NMR spectrum of compound **3** in $CDCl_3$ by the detection of two broadened quartets for the N–CH_2 protons at 4.05 ppm and 3.73 ppm and two overlapping triplets for the CH_3 protons in the region of 1.36–1.40 ppm. The ^{125}Te resonance of **3** appears at 855.2 ppm, which corresponds to a high-field shift of about 350 ppm compared to the signal detected for compound **1**, but still falls into the common range of Te(II) compounds.[48–51] The ESI(+) MS spectrum of **3** shows a low-intensity molecular ion peak for $[M+Na]^+$ at m/z = 705.9697. The most intense tellurium-containing fragment appears at m/z = 524.0441 and can be assigned to $[M - HBr - Br]^+$.

X-ray structure determinations on **3** and **4** confirm the conclusions drawn from the spectroscopic data. Structural plots are shown in Figure 2 and selected bond lengths and angles are summarized in Tables 2 and 3.

H_2L^{Et} acts as a neutral ligand in both compounds and coordinates to tellurium via the two sulfur donors. The

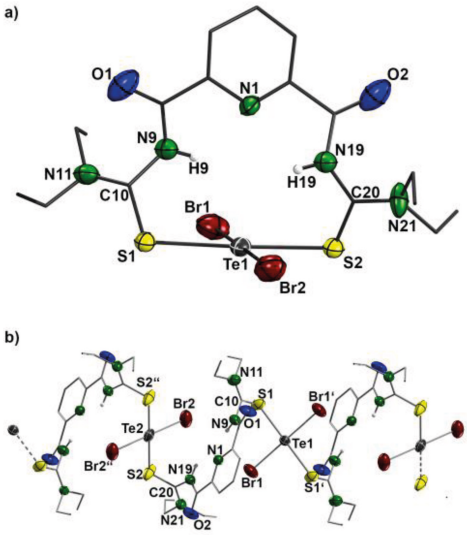

Figure 2. Molecular structures of a) compound **3** and b) of the coordination polymer **4**. Hydrogen atoms (except of the amide H atoms) are omitted for clarity. Thermal ellipsoids are shown with 50 per cent probability.

Table 2. Selected bond lengths/Å and angles/° in compound **3**.[a]

Te1–S1	2.770(7) 2.797(7)	Te1–S2	2.646(7) 2.637(7)	Te1–Br1	2.763(4) 2.735(4)
Te1–Br2	2.644(4) 2.637(7)	S1–C10	1.77(3) 1.77(3)	S2–C20	1.72(3) 1.69(3)
C10–N9	1.43(3) 1.39(3)	C10–N11	1.31(3) 1.33(3)	C20–N19	1.39(3) 1.41(3)
C20–N21	1.35(3) 1.31(4)	Te1–S1–C10	99.8(10) 96.4(9)	Te1–S2–C20	115(2) 122(2)
S1–C10–N9	115(2) 122(2)	S2–C20–N19	124(2) 118.6(2)	S1–Te1–S2	175.9(2) 176.9(2)
Br1–Te1–Br2	177.7(1) 177.6(1)				

[a] Values for two independent species.

Research Article
doi.org/10.1002/ejic.202400344

Table 3. Selected bond lengths/Å and angles/° in compounds **4**.

Te1–S1	2.657(1)	Te1–Br1	2.7352(6)	Te2–S2	2.698(2)
Te2–Br2	2.7173(7)	S1–C10	1.694(5)	S2–C20	1.711(5)
C10–N9	1.387(6)	C10–N11	1.305(6)	C20–N19	1.388(6)
C20–N21	1.307(6)	Te1–S1–C10	104.0(2)	Te2–S2–C20	108.7(2)
S1–C10–N9	118.3(4)	S2–C20–N19	118.6(4)	S2–Te1–S1′	180
Br1–Te1–Br1′	180				

(′) symmetry operation: -x,1-y,1-z.

coordination situation in **3** is very similar to that already described for compound **2**, except that the coordination environment of the tellurium atom is not T-shaped but square planar with the sulfur atoms of H_2L^{Et} in *trans* positions to each other. The average values of the *trans* angles S1–Te1–S2 or Br1–Te1–Br2 (values for two crystallographically independent species) deviate from the ideal values by only 3.9(2)° and 2.1(2)°, respectively. While the respective Te–S and Te–Br bond lengths in the polymeric compound **4** are similar, the corresponding values in both crystallographically independent species of the monomer **3** are pairwise different, indicating each two shorter and two longer Te–S and Te–Br bonds. This point, however, should not be matter of a more detailed discussion since artifacts coming from the relatively low quality of the corresponding X-ray structure determination cannot be excluded and we unfortunately failed in growing better single crystals.

The pyridine N atom of H_2L^{Et} is situated exactly in the direction of one lone pair of the tellurium atom with the N1–Te1–X angles (where X=S1, S2, Br1, Br2) being very close to 90°. As in the structurally related tellurium(II)-containing cation in **2**, the average N1–Te1 distance of 3.969(2) Å in compound **3** is too long to conclude any interactions between nitrogen and tellurium. Nevertheless, the distance between the two atoms, combined with their respective geometric arrangement, is remarkably short with regard to the presence of the lone pairs of both the pyridine nitrogen and the tellurium atoms.

We therefore performed DFT calculations on the B3LYP/def2-TZVPD level in the gas phase to illuminate the electronic situation in the resulting lone-pair-filled cavities. After geometry optimization, the electronic structure within the compounds was assessed by a second-order perturbation analysis based on natural bond orbitals (NBOs), electron localization function (ELF), the quantum theory of atoms in molecules (QTAIM) and the reduced density gradient (RDG), see Figure 3.

Firstly, the two lone-pairs are clearly directional and of essentially *p*-character for tellurium and sp^2-character for nitrogen. Secondly, they are oriented directly opposite of each other and an RDG map (see Supporting Information) indicates a weak van der Waals contact in the center of the Te,H,H,N ring. It becomes obvious from the deformation of the orbital shape, that the lone pair of the tellurium atom interacts much more pronounced with the N–H anti-bonding orbital than the lone-pair of the pyridine nitrogen atom. The deformation is also obvious from the ELF map in the Te,H,H plane, while the lone-pair of the pyridine nitrogen atom is basically undisturbed by the neighboring N–H hydrogen atoms. The graphical difference is also reflected quantitatively in the respective second order perturbation energies of ca. 7 kcal/mol for the Te(II)···H interactions in **3** (6 kcal/mol for Te(II) in **2**), while it is ca. 3 kcal/mol for the N···H interactions. Like the situation in compound **3** and the cation of compound **2**, DFT calculations on the B3LYP/def2-TZVPD level for compound **1** also show a much more pronounced orbital interaction to the bromide compared to the central pyridine nitrogen atom (5 kcal/mol *versus* 2 kcal/mol). The involved orbitals are visualized in the Supplementary Material.

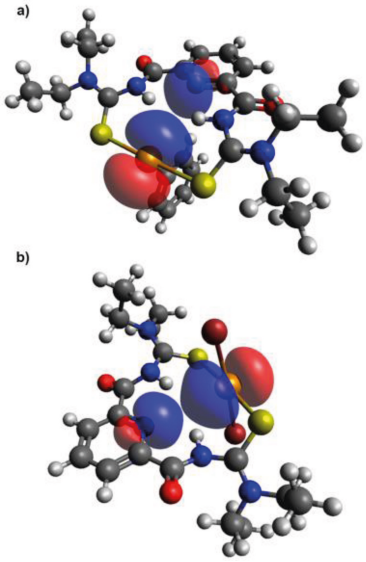

Figure 3. Gas-phase optimized structures of a) the cation of compound **2** showing the pyridine nitrogen lone pair (HOMO-14) as well as the lone pair of tellurium(II) oriented towards the pyridine ring (HOMO-15) and b) of compound **3** showing the pyridine nitrogen lone pair (HOMO-12) as well as the lone pair of tellurium(II) oriented towards the pyridine ring (HOMO-13). Orbitals are plotted at 0.04 a.u.

Topologically, (+3,−1) critical points are located along the interaction paths in **3** indicating bonding interactions, while (+3,+1) or "ring" critical points suggest a closed, circular electronic structure within the Te,H,H,N ring as well as the rings spun by the pyridine nitrogen atom *via* the carbon-tethered N–H units. The existence of topological (+3,−1) critical points and the electronic properties at those points are consistent with corresponding criteria for hydrogen bonding interactions

Research Article
doi.org/10.1002/ejic.202400344

such as an electron density in the range 0.002 a.u. $< \rho_{A\cdots H\text{-}D} <$ 0.040 a.u. ($\rho_{Te\cdots H} = 0.012$ and 0.013 a.u.; $\rho_{N\cdots H} = 0.017$ a.u.) and a Laplacian of the electron density in the range 0.024 a.u. $< \nabla^2(\rho)_{A\cdots H\text{-}D} < 0.139$ a.u. ($\nabla^2(\rho)_{Te\cdots H} = 0.056$ and 0.057 a.u.; $\nabla^2(\rho)_{N\cdots H} = 0.092$ and 0.095 a.u.). The interactions can further be classified as weak as both $\nabla^2(\rho)_{A\cdots H\text{-}D}$ and the energy density $H(\rho)_{A\cdots H\text{-}D}$ are small positive numbers and the absolute of the potential energy density $V(\rho)_{A\cdots H\text{-}D}$ is smaller than the extend of the Lagrangian (or local) kinetic energy density $G(\rho)_{A\cdots H\text{-}D}$. The energy of the hydrogen bonds can be estimated as roughly $^1/_2 V(\rho)_{A\cdots H\text{-}D}$ and hence, the Te···H H-bond energy is lower with roughly 13 kJ/mol compared to the N···H-bond energy, which is between 23 and 24 kJ/mol after conversion from atomic units. The discrepancy between the NBO considerations and the binding energy is most likely attributed to the forced localization of orbitals in NBO for this highly delocalized molecule and hence, the energies obtained from the topological description are supposedly more reliable. Further details, graphic depictions and the corresponding references for the applied criteria are given as Supporting Information. Attempts to derive details about the observed NMR spectra by means of computational methods did not deliver satisfactory results.

The results of the single-crystal X-ray diffraction analysis of compound **4** verify its polymeric nature with the chemical composition of $[Te^{II}Br_2(H_2L^{Et})]_\infty$. Figure 2b depicts the helical arrangement of the monomeric units, in which the tellurium atoms are placed on inversion centers and bind to two Br^- ligands and the sulfur atoms of two different H_2L^{Et} ligands. Although the coordination model in the two neighboring $\{TeS_2Br_2\}$ units are identical, some differences in their Te–Br and Te–S bond lengths are observed. The protonation of the amide nitrogen atoms N9 and N19 is confirmed by the detection of electron density on the respective positions in the final Fourier map, which could be successfully refined as hydrogen atoms. These hydrogen atoms contribute to weak intramolecular hydrogen bonds such as N9–H9···N1, N9–H9···Br1 and N19–H19···Br2, which stabilize the helical structure of **4**. The carbon-oxygen distances of 1.202(6) and 1.216(6) Å are in the typical range of C=O double bonds. The C10–S1 and C20–S2 bonds of 1.694(5) and 1.711(5) Å are slightly elongated from typical C=S double bonds due to the formation of the sulfur-tellurium bonds.

The bonding between the halogen and chalcogen atoms and the tetragonal or trigonal tellurium atoms can easily be distinguished into chalcogen, ionic and covalent bonds based on the localized orbital locator (see Experimental for references and Supporting Information for details). The trigonal tellurium atom in **2**, thus, shows a covalent bond to C, a polar covalent bond to one of the sulfur atoms and a chalcogen bond is established to the second sulfur atom. Similarly, the tetragonal tellurium atom in **3** shows a covalent bond to one bromine atom and one covalent polarized bond to one of the sulfur atoms, while the interaction with both other donor atoms can be understood in terms of chalcogen bonding. A similar situation is found for **1**, where two polar covalent Te–Br bonds can be identified and chalcogen bonding is established between tellurium and sulfur as well as one bromine donor atom. The chalcogen bonds in compounds **1**, **2** and **3** are strong according to their solid-state bonding parameters and show a relatively strong bond contraction of −30%, whereas the average for Te···Br is −9% and for Te···S is −18% (see Experimental for references and Supporting Information for details).

Mixed-Metal Complexes

In the preface of the present article, compounds of the type H_2L^R were introduced as ambivalent ligands with a donor atom constellation, which enables them to establish coordinative bonds to various metal ions depending on their 'softness' or 'hardness' according to Pearson's concept. Irrespective of the oxidation state of tellurium, we found exclusively coordination to the sulfur atom(s). We could also not isolate any pure product during our attempts to bind a second $PhTeBr_3$ unit to the uncoordinated thiourea unit in compound **1**. Obviously, the reduction of tellurium and an *S,S* coordination of the resulting Te(II) unit is preferred as has been found in compounds **2**–**4**.

The previously reported ready formation of mixed-metal complexes with H_2L^R ligands[37–44] led us to perform experiments between H_2L^{Et} with mixtures of $PhTeX_3$ (X=Br, I) and divalent metal ions such as Ni^{2+}, Co^{2+}, Cu^{2+} or Mn^{2+}. They gave colored products of the composition $[M(PhTe)(H_2L^{Et}{}_2\text{-}S,S)][PhTeX_4]$ in clean reactions and with good yields (Scheme 5). The corresponding bromido derivatives can also be obtained from direct reactions from **1** and the corresponding metal acetate. Since the purity of the products and the obtained yield are similar, there is a clear preference for the simple one-pot reaction in methanol.

The elemental analyses of the products fit with an approximate composition of '$[M(PhTe)(H_2L^{Et}{}_2\text{-}S,S)][PhTeX_4]$'. Interestingly, in the IR spectra of the products two strong absorptions at 1710 cm^{-1} and 1680 cm^{-1} are still present, which is the typical region of the vibrations of uncoordinated C=O groups in the monodentate *S*-bonded benzoylthiourea

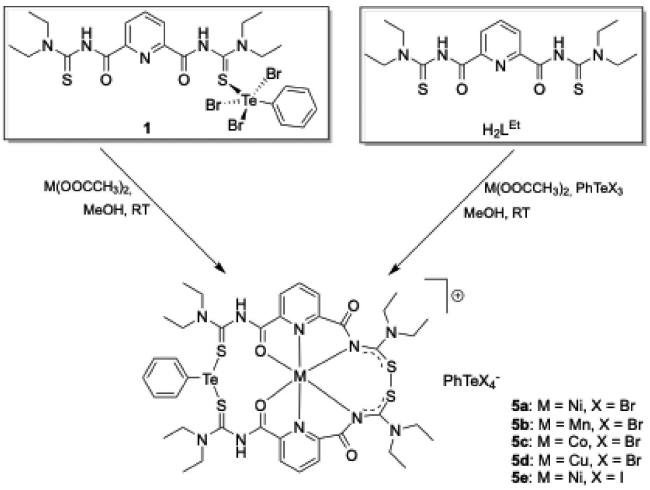

Scheme 5. Reactions of H_2L^{Et} with $PhTeX_3$ (X=Br, I) and $M(OOCCH_3)_2$ salts.

Research Article
doi.org/10.1002/ejic.202400344

complexes.[37,52] These stretches are much higher than the values found for *S,O*-chelating benzoylthioureato complexes, which appear around 1550 cm^{-1}.[23,24,53] While the ESI(+) mass spectra of the obtained mixed-metal complexes show peaks for $[M(PhTe)(H_2L^{Et}{}_2\text{-}S,S)]^+$ cations, the corresponding negative mode ESI spectra give clear evidence for the presence of $[PhTeX_4]^-$ anions.

Single crystal X-ray diffraction studies provided proof for the composition of the mixed-metal products. Figure 4 shows the structure of the complex cation of the nickel compound of $[Ni(PhTe)(H_2L^{Et}{}_2\text{-}S,S)][PhTeI_4]$ (**5 e**) and Table 4 contains selected bond lengths and angles of the complex cation.

Analogous structures could also be derived from X-ray structure determinations on the nickel complex $[Ni(PhTe)(H_2L^{Et}{}_2\text{-}S,S)][PhTeBr_4]$ (**5 a**) and the corresponding cobalt compound **5 c**. The limited quality of the single crystal measurements on **5 a** and **5 c** did not allow an anisotropic refinement of the resulting data sets, but gave an unambiguous confirmation of their structures. Consequently, no detailed discussion about the bond lengths and angles in these two products shall be included here and the data are also not submitted for deposit in the CSD database. Nevertheless, they are supplied as structural plots and full lists of bond lengths and angles in the Supporting Information.

The products contain an unprecedented $\{H_2L^{Et}{}_2\text{-}S,S\}^{2-}$ ligand system consisting of two 'half-oxidized' H_2L^{Et} aroylthioureas, which coordinate to M^{2+} ions with the two pyridine nitrogen atoms, two amide N atoms and two oxygen atoms. Two of the sulfur atoms bind to a $\{PhTe\}^+$ unit similarly to the situation found in compound **2**, while the remaining two sulfur atoms establish a disulfide bond. The detection of a (partial) oxidation product of H_2L^{Et} as a ligand in compound **5** supports the assumption that the formation of compounds **2**, **3** and **4** may also proceed *via* disulfide intermediates.

The newly formed ligand $\{H_2L^{Et}{}_2\text{-}S,S\}^{2-}$ surrounds the central M^{2+} ions as a hexadentate chelator using the two pyridine N atoms, the amide *N* atoms of oxidized arms and the carboxamide *O* atoms of the non-oxidized arms. Thus, this hexadentate chelator system consists of two *O,N,N* pincer moieties, which are extendedly linked by a formally seven-membered chelate ring comprised of the Ni1, N19, C20, S2, S3, C40 and N39. The bonding situation in the $[PhTeI_4]^-$ counter ions is structurally unexceptional and corresponds to the few other examples of structurally characterized $[PhTeI_4]^-$ salts.[12,54–60]

In order to prevent the oxidation of the thiourea groups, the Te(II) precursor 'TePhI' was used to synthesize the mixed-metal complex. Phenyltellurium(II) iodide is a tetrameric compound, which can readily be generated *in situ* by the reaction of $(PhTe)_2$ with elemental iodine.[61] The corresponding nickel(II) complex was synthesized by the addition of $Ni(CH_3COO)_2 \cdot 4\ H_2O$ to a solution of H_2L^{Et} and 'TePhI' in methanol. The molar ratio Ni^{2+}/H_2L^{Et} was kept at 1:2 to rationalize the expected octahedral coordination of the Ni^{2+} ion by two pyridine-2,6-dicarboxamide moieties, while the amount of the tellurium-containing starting material was kept constant. Under such conditions, only a small amount of a precipitate with the chemical composition of $[Ni(PhTe\text{-}\mu\text{-}I\text{-}TePh)_2(L^{Et})_2]$ (**6**) could be isolated from the reaction mixture. The use of four equivalents of 'PhTeI' per Ni^{2+}, however, resulted in the isolation of the product in high yields (Scheme 6), which is easily understood when regarding the structure of the product.

The IR spectrum of **6** closely resembles those obtained for the compounds of type **5**. The disappearance of the absorption in the region around 3100 cm^{-1} and the presence of a strong absorption at 1636 cm^{-1} indicate the deprotonation of NH-amide groups and the existence of non-bonded C=O groups, respectively.

Single crystals of **6** suitable for X-ray diffraction were obtained by slow evaporation of a $MeOH/CH_2Cl_2$ solution. Figure 5 illustrates the molecular structure of **6**. Selected bond

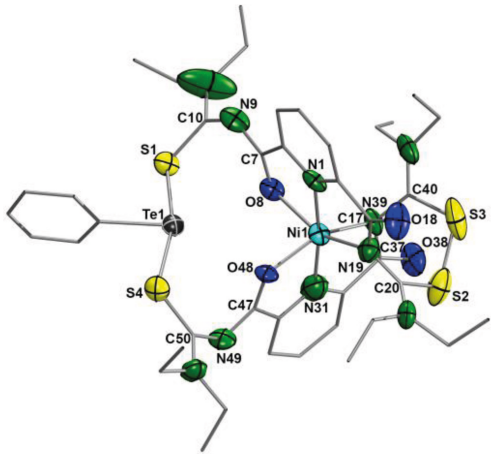

Figure 4. Structure of the $[Ni(PhTe)(H_2L^{Et}2\text{-}S,S)]^+$ cation of compound **5 e**. Hydrogen atoms are omitted for clarity. Thermal ellipsoids are shown with 50 per cent probability.

Table 4. Selected bond lengths/Å and angles/° in the complex cation of compound (**5 e**).Values are given for two independent molecules.

Te1–S1	2.718(4) 2.714(4)	Te1–S4	2.649(6) 2.631(4)	S1–C10	1.70(2) 1.65(2)
S4–C50	1.71(2) 1.72(1)	Ni1–N1	1.98(2) 1.97(1)	Ni1–N31	1.98(1) 1.95(2)
Ni1–O8	2.088(9) 2.078(9)	Ni1–O48	2.12(1) 2.11(1)	Ni1–N19	2.15(1) 2.15(1)
Ni1–N39	2.14(1) 2.18(1)	C7–O8	1.25(2) 1.24(2)	C47–O48	1.22(2) 1.19(2)
C17–O18	1.24(2) 1.24(2)	C37–O38	1.24(2) 1.19(2)	C20–S2	1.80(2) 1.80(2)
C40–S3	1.80(2) 1.78(2)	S2–S3	2.016(9) 2.018(7)		
Te1–S1–C10	110.3(6) 107.9(5)	Te1–S4–C50	107.6(6) 107.2(5)	S1–Te1–S41	166.3(1) 166.3(1)
C20–S2–S3	104.1(7) 102.9(5)	C40–S3–S2	99.2(6) 102.0(6)		

Research Article
doi.org/10.1002/ejic.202400344

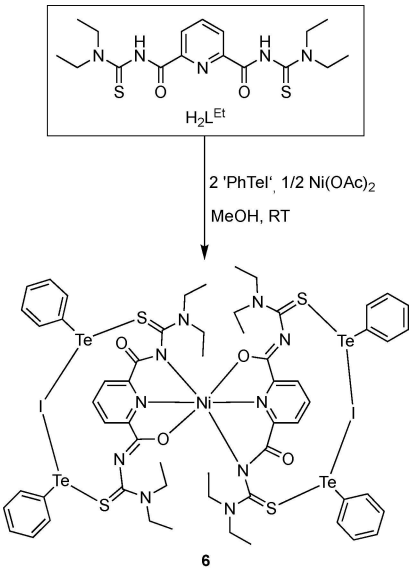

Scheme 6. Reactions of H_2L^{Et} with 'PhTeI' and $Ni(CH_3COO)_2 \cdot 4\,H_2O$.

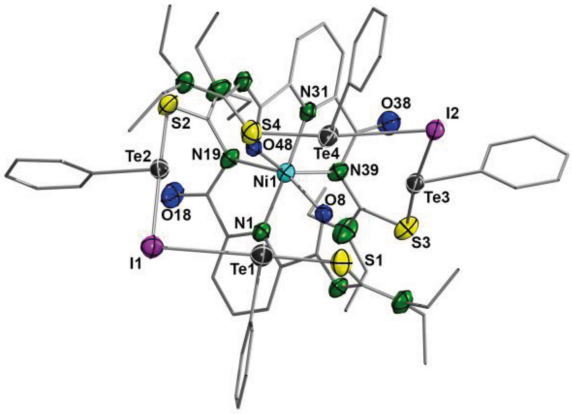

Figure 5. Structure of $[Ni(PhTe\text{-}\mu\text{-}I\text{-}TePh)_2(L^{Et})_2]$ (**6**). Hydrogen atoms are omitted for clarity. Thermal ellipsoids are shown with 50 per cent probability.

lengths and angles are contained in Table 5. The molecular structure of **6** confirms that the aroylthiourea ligand is not oxidized. Similar to the bonding situation in the compounds of type **5**, the nickel atom in **6** is octahedrally coordinated by *O,N,N* donor sets of two pyridine-2,6-dicarboxamide moieties, each of which belongs to one $\{L^{Et}\}^{2-}$ unit. The atoms within each pincer unit and the nickel atom are almost coplanar with a main deviation of 0.176(7) Å from a mean least squares plane for the non-coordinating O18 and O38 atoms. This planarity is also extended to the carbon atoms of thiocarbonyl groups. However, the sulfur atoms of the two thiocarbonyl groups are turned away with an average S=C–N–CO torsion angle of 64.4° and placed on the same side of the plane. Each of the sulfur atoms is bonded to one $\{PhTe\}^+$ core, while each two of the $\{PhTe\}^+$ cores are bridged by an iodido ligand. Accordingly, a T-shape structure best describes the coordination geometry around the tellurium atom.

The Te–S bond lengths relating to S atoms in the *O*-bonded aroylthiourea arms are shorter than those in the *N*-bonded aroylthiourea subunits. This finding is accompanied by unequal Te–I bond distances. Particularly, the longer the Te–S bond, the shorter is the corresponding Te–I bond. This structural feature is a good evidence for the partial localization of negative charge on the N atom of the *N*-bonded aroylthiourea site more than on the S atom of the *O*-bonded aroylthiourea site. Nevertheless, the delocalization of the negative charges over the ligand skeleton is reasonable and responsible for the analogous C–O, C–N and C–S bond distances in the two aroylthiourea subunits independent of the coordination modes.

Conclusions

2,6-Dipicolinoylbis(*N*,*N*-dialkylthioureas) are versatile ligands, which form stable complexes with tellurium(II) and tellurium(IV) building blocks *via* their sulfur donor atoms. The bonding situation inside the organic ligand manifests in a wide variety of coordination modes, including neutral monodentate *S*-bonded, neutral bidentate *S*-bonded or neutral/negative monodentate *S*-bonded motifs. The coordination sphere of the tellurium atoms can be controlled by both the reaction conditions and/or the tellurium-containing precursor. Reduction of Te(IV) starting materials by the used thioureas is a common feature of such reactions. The addition of *3d* transition metal ions to reaction mixtures containing 2,6-dipicolinoylbis(*N*,*N*-dialkylthioureas) and Te(IV) or Te(II) starting materials results in the formation of hetero bimetallic products with central transition metal ions and peripheral tellurium units.

Table 5. Selected bond lengths/Å and angles/° in compound **6**.

Ni1–N1	1.984(5)	Ni1–N31	1.976(4)	Ni1–N19	2.179(4)
Ni1–N39	2.188(5)	Ni1–O8	2.127(4)	Ni1–O48	2.139(4)
Te1–S1	2.458(2)	Te1–I1	3.371(2)	Te2–S2	2.528(2)
Te2–I1	3.199(2)	Te3–S3	2.466(2)	Te3–I2	3.119(1)
Te4–S4	2.544(2)	Te4–I2	3.341(1)		
S1–Te1–I1	178.54(5)	S2–Te2–I1	176.66(5)	S3–Te3–I2	174.86(4)
S4–Te4–I2	172.77(5)	Te1–I1–Te2	83.70(6)	Te3–I2–I4	88.17(6)

Research Article
doi.org/10.1002/ejic.202400344

Experimental Section

All chemicals used in this study were reagent grade and used without further purification. Solvents were dried and used freshly distilled unless otherwise stated. The ligand H_2L^{Et},[35] $TeBr_4$,[62] $PhTeBr_3$,[63] $PhTeI_3$,[64] and *in situ* formed PhTeI[61] were prepared by standard procedures.

Infrared spectra were measured as KBr pellets on a Shimadzu FTIR-spectrometer between 400 and 4000 cm^{-1}. NMR spectra were taken with JEOL 400 MHz multinuclear spectrometer. ESI mass spectra were measured with an Agilent 6210 ESI-TOF (Agilent Technology) mass spectrometer. All MS results are given in the form *m/z* assignment. Elemental analysis of carbon, hydrogen, nitrogen, and sulfur were determined using a Heraeus vario EL elemental analyzer.

Crystallography

The intensities for the X-ray determinations were collected on STOE IPDS 2T or Bruker instruments with Mo Kα radiation (λ = 0.71073 Å). Standard procedures were applied for data reduction and absorption correction.[65,66] Structure solution and refinement were performed with SHELX[67,68] included in the WINGX and OLEX2 program packages.[69,70] Hydrogen atoms were calculated for idealized positions and treated with the "riding model" option of SHELXL unless otherwise stated. DIAMOND was used to prepare the structure representations.[71] More details about the data collections, the structure calculations and ellipsoid representations of the crystal structures are provided in the following tabular material. The structural data are deposited with the Cambridge Crystallographic Data Centre with the deposition numbers CCDC-2322091 ([$PhTeBr_3(H_2L^{Et})$]), CCDC-2322092 ([$PhTe(H_2L^{Et})$][$PhTeBr_4$]), CCDC-2322093 ([$TeBr_2(H_2L^{Et})$]), CCDC-2322094 ([$TeBr_2(H_2L^{Et})]_\infty$), CCDC-2322095 ([$PhTe(H_2L^{Et}$-*S*,*S*)Ni][$PhTeI_4$]) and CCDC-2322096 ([$Ni(PhTe$-$\mu$-I-$TePh)_2(L^{Et})_2$]).[72].

Syntheses

*[$PhTeBr_3(H_2L^{Et})$] (**1**)*: H_2L^{Et} (40 mg, 0.1 mmol) was added to a solution of $PhTeBr_3$ (45 mg, 0.1 mmol) in 5 mL of MeOH. The reaction mixture was stirred at room temperature for 1 h. A yellow solid (compound **1**) deposited, which was collected by filtration and washed with MeOH. Single crystals of **1** suitable for X-ray diffraction were obtained by slow evaporation of a CH_2Cl_2/MeOH (1/1 v/v) solution. A few single crystals of a side product (compound **2**) were harvested from the mother liquor after standing for several days at room temperature and slow evaporation of the solvent. Yield: 60 mg (72 %). Elemental analysis: Calcd. for $C_{23}H_{30}N_5O_2S_2Br_3Te$: C, 32.9; H, 3.6; N, 8.3; S, 7.6 %. Found: C, 33.1; H, 3.6; N, 8.3; S, 7.5 %. IR (cm^{-1}): 3139 (m, br), 2968 (w), 2934 (w), 2872 (w), 1709 (s), 1680 (s), 1543 (s), 1523 (s), 1436 (s, br), 1376 (w), 1283 (m), 1121 (m), 1100 (m), 1070 (m), 1000 (w), 884 (m), 735 (m), 646 (m), 552 (w). ^{1}H NMR (400 MHz, $CDCl_3$, ppm): 10.25 (br, 2H, NH), 8.56 (dd, *J* = 7.0 Hz, *J* = 3,0 Hz, 2H, Ph), 8.45 (d, *J* = 8.0 Hz, 2H, Py), 8.17 (t, *J* = 8.0 Hz, 1H, Py), 7.34 (m, 3H, Ph), 4.05 (q, br, *J* = 6.8 Hz, 4H, CH_2), 3.69 (q, br, *J* = 6.8 Hz, 4H, CH_2), 1.41 (t, br, *J* = 8.3 Hz, 6H, CH_3), 1.39 (t, br, *J* = 8.3 Hz, 6H, CH_3). ^{13}C NMR ($CDCl_3$, ppm): 177.0 (C=S), 159.2 (C=O), 147.3 (C_{Ar}, *o*-py), 140.1 (C_{Ar}, *p*-py), 135.6 (C_{Ph}, *o*-Te), 131.0 (C_{Ph}, *p*-Te), 129.4 (C_{Ph}, *m*-Te), 127.7 (C_{Ar}, *m*-py), 49.2 (CH_2), 48.5 (CH_2), 13.5 (CH_3), 11.9 (CH_3). ^{125}Te NMR ($CDCl_3$, ppm): 1204.3. ESI(+) MS (m/z): 600.0755 [M - 2HBr - Br)]$^+$ (calc. 600.0747).

*[$PhTe(H_2L^{Et})$][$PhTeBr_4$] (**2**)*: A small amount of pale yellow crystals of compound **2** was obtained by slow concentration of the mother liquor obtained from the synthesis of compound **1** after removal of the main product by filtration. Somewhat larger yields of **2** are obtained when a slight excess of H_2L^{Et} (approximately 2 equivalents) is used and the reaction mixture is heated on reflux for 5 min. Yield: 3.2 mg (5.5 % based on $PhTeBr_3$). Elemental analysis: Calcd. for $C_{31}H_{41}Br_4N_5O_2S_2Te$: C, 36.3; H, 4.0; N, 6.8; S, 6.2 %. Found: C, 36.4; H, 4.1; N, 6.8; S, 6.3 %. IR (cm^{-1}): 3189 (m), 3025 (w), 2982 (w), 2970 (w), 1725 (s), 1557 (s), 1474 (s, br), 1379 (w), 1357 (w), 1285, m), 1219 (m), 1126 (m),1079 (m), 998 (w), 737 (m), 679 (w), 455 (w).

*[$TeBr_2(H_2L^{Et})$] (**3**)*: H_2L^{Et} (120 mg, 0.3 mmol) was added to a suspension of $TeBr_4$ (45 mg, 0.1 mmol) in 5 mL of MeOH. The reaction mixture was stirred at room temperature, which resulted in the gradual formation of a clear solution and the subsequent precipitation of an orange-red solid. After 1 h, this solid (compound **3**) was collected by filtration. Single crystals of **3** suitable for X-ray diffraction were obtained by slow evaporation of a solution of the complex in CH_2Cl_2/MeCN (9/1 v/v). Yield: 60 mg (88 %) based on $TeBr_4$. Elemental analysis: Calcd. for $C_{17}H_{25}N_5O_2S_2Br_2Te$: C, 29.9; H, 3.7; N, 10.2; S, 9.4 %. Found: C, 29.3; H, 3.7; N, 9.9; S, 9.1 %. IR (cm^{-1}): 3193 (w, br), 2975 (w), 2932 (w), 2872 (w), 1715 (s), 1555 (s), 1460 (s, br), 1380 (w), 1289 (m), 1221 (s), 1179 (w), 1092 (m), 1127 (m), 1992 (m), 1074 (m), 1002 (w), 873 (m), 754 (m), 695 (w), 627 (w). ^{1}H NMR (400 MHz, $CDCl_3$, ppm): 10.48 (br, 2H, NH), 8.42 (d, *J* = 7.8 Hz, 2H, Py), 8.13 (t, *J* = 8.0 Hz, 1H, Py), 4.05 (q, br, *J* = 7.6 Hz, 4H, CH_2), 3.73 (q, br, 4H, CH_2), 1.39 (t, br, 6H, CH_3), 1.37 (t, br, 6H, CH_3). ^{13}C NMR ($CDCl_3$, ppm): 177.1 (C=S), 159.5 (C=O), 147.8 (C_{Ar}, *o*-py), 140.1 (C_{Ar}, *p*-py), 127.2 (C_{Ar}, *m*-py), 49.3 (CH_2), 48.6 (CH_2), 13.6 (CH_3), 11.8 (CH_3). ^{125}Te NMR ($CDCl_3$, ppm): 855.2. ESI(+) MS (m/z): 524.0441 [M - HBr -Br)]$^+$ (calc. 524.0434).

*[$TeBr_2(H_2L^{Et})]_\infty$ (**4**)*: Orange-red plates of the polymeric compound $[TeBr_2(H_2L^{Et})]_\infty$ (**4**) were obtained by keeping the clear mother liquor obtained from the synthesis of **3** for several days at room temperature. Yield: 6.0 mg (9.0 % based on $TeBr_4$). Elemental analysis: Calcd. for $C_{17}H_{25}N_5O_2S_2Br_2Te$: C, 29.9; H, 3.7; N, 10.2; S, 9.4 %. Found: C, 29.5; H, 3.7; N, 10.0; S, 9.2 %. IR (cm^{-1}): 3256 (w), 3077 (w), 2974 (w), 2936 (w), 1711 (s), 1541 (s), 1460 (s, br), 1420 (m), 1375 (m), 1343 (w), 1286 (m), 1229 (s), 1208 (s), 1123 (m), 1093 (m), 1081 (m), 1066 (m), 999 (m), 874 (m), 838 (m), 751 (m), 669 (m), 645 (m), 587 (w), 541 (w), 494 (w). The formation of compound **4** is also observed during the reaction of H_2L^{Et} with $Pb(CH_3COO)_2$ and by subsequent heating of solutions of compound **3.**

*[$PhTe(L^{Et}$-*SS*)Ni][$PhTeBr_4$] (**5a**)*: Method 1. A solution of Ni-$(CH_3COO)_2\cdot 4\ H_2O$ (6.3 mg, 0.25 mmol) in 3 mL MeOH was added to a solution of **1** (42.0 mg, 0.5 mmol) dissolved in 5 mL CH_2Cl_2/MeOH (1/1 v/v). The mixture was stirred at room temperature. After a few minutes, a greenish-yellow solid started to precipitate. The stirring was continued for 1 h without additional heating, the resulting solid was filtered off and washed with cold MeOH.

Method 2. Solid H_2L^{Et} (200 mg, 0.51 mmol) was added to a solution of $PhTeBr_3$ (225 mg, 0.5 mmol) in 5 mL MeOH. The mixture was stirred at 45 °C for 10 min to obtain a clear yellow solution. $Ni(CH_3COO)_2\cdot 4\ H_2O$ (63 mg, 0.25 mmol) in 5 mL MeOH was added dropwise. A greenish-yellow solid quickly deposited. The mixture was stirred for 1 h without heating. The resulting solid was filtered off and washed with cold MeOH.

Method 3. Solid H_2L^{Et} (200 mg, 0.51 mmol) was added to a solution of $Ni(CH_3COO)_2\cdot 4\ H_2O$ (63 mg, 0.25 mmol) in 5 mL MeOH. The mixture was stirred at room temperature for 10 min giving a bright green solution. $PhTeBr_3$ (225 mg, 0.5 mmol) dissolved in 5 mL MeOH was added dropwise. A greenish-yellow solid quickly

Research Article
doi.org/10.1002/ejic.202400344

precipitated. The stirring was continued for 1 h without additional heating. The resulting solid was filtered off and washed with cold MeOH.

Single-crystals of **5a** suitable for X-ray diffraction were obtained by slow evaporation of a CH_2Cl_2/MeCN (9/1 v/v) solution. Yield: 322 mg (82%). Elemental analysis: Calcd. for $C_{46}H_{56}Br_4N_{10}NiO_4S_4Te_2$, C, 35.1; H, 3.6; N, 8.9%. Found: C, 34.1; H, 3.6; N, 8.2%. IR (KBr, cm^{-1}): 2978 (w), 2934 (w), 2362 (w), 1724 (s), 1647 (w), 1556 (s), 1434(s), 1384 (m), 1355 (m), 1285 (m), 1239 (m), 1149 (w), 1076 (m), 841 (w), 739 (m, br), 679 (m), 456 (w). MS ESI(+) (m/z): 1051.1387 (M^+) (calc. 1051.1393).

[PhTe(L^{Et}_2-SS)Mn][PhTeBr$_4$] (***5b***): The compound was prepared as described for **5a**, but with $Mn(CH_3COO)_2 \cdot 4\ H_2O$ instead of $Ni(CH_3COO)_2 \cdot 4\ H_2O$. The compound was isolated as a yellow crystalline solid. Yield 254 mg (65%). Elemental analysis: Calcd. for $C_{46}H_{56}Br_4N_{10}MnO_4S_4Te_2$, C, 35.2; H, 3.6; N, 8.9%. Found: C, 34.9; H, 3.4; N, 8.0%. IR (KBr, cm^{-1}): 2978 (w), 2936 (w), 1710 (s), 1683 (s), 1545 (s), 1459(s, br), 1378 (w), 1355 (w), 1285 (m), 1234 (m), 1123 (m), 1073 (m), 1000 (w), 916 (w), 884 (w), 839 (w), 794 (m), 680 (m, br), 456 (w). MS ESI(+) (m/z): 1048.1481 (M^+) (calc. 1048.1420).

[PhTe($H_2L^{Et}_2$-S,S)Co][PhTeBr$_4$] (***5c***): The compound was prepared as described for **5a**, but with $Co(CH_3COO)_2 \cdot 4\ H_2O$ instead of $Ni(CH_3COO)_2 \cdot 4\ H_2O$. The compound was isolated as a yellow-orange crystalline solid. Yield 276 mg (70%). Elemental analysis: Calcd. for $C_{46}H_{56}Br_4N_{10}CoO_4S_4Te_2$, C, 35.1; H, 3.6; N, 8.9%. Found: C, 34.6; H, 3.6; N, 8.5%. IR (KBr, cm^{-1}): 2974 (m), 2933 (w), 1711 (w), 1646 (s), 1562 (s), 1508 (s), 1434(m), 1395 (s), 1346 (m), 1168 (m), 916 (w), 875 (w), 760 (m), 740 (m), 669 (m), 458 (w). MS ESI(+) (m/z): 1052.1355 (M^+) (calc. 1052.1372).

[PhTe($H_2L^{Et}_2$-S,S)Cu][PhTeBr$_4$] (***5d***)*:* The compound was prepared as described for **5a**, but with $Cu(CH_3COO)_2 \cdot 2\ H_2O$ instead of $Ni(CH_3COO)_2 \cdot 4\ H_2O$. The compound was isolated as a dark green, crystalline solid. Yield 205 mg (52%). Elemental analysis: Calcd. for $C_{46}H_{56}Br_4N_{10}CuO_4S_4Te_2$, C, 35.0; H, 3.6; N, 8.9%. Found: C, 34.3; H, 3.5; N, 8.3%. IR (KBr, cm^{-1}): 2977 (w), 1710 (s), 1682 (s), 1544 (s), 1459 (s, br), 1378 (m), 1285 (m), 1231 (m, br), 1122 (m), 1100 (m), 1074 (m), 1000 (w), 839 (w), 737 (m), 681 (m), 455 (w). MS ESI(+) (m/z): 1056.1346 $(M)^+$ (calc. 1056.1336).

[PhTe($H_2L^{Et}_2$-S,S)Ni][PhTeI$_4$] (***5e***): The compound was prepared as described for **5a**, but with $PhTeI_3$ instead of $PhTeBr_3$. The compound was isolated as a yellow crystalline solid. Yield 384 mg (87%). Elemental analysis: Calcd. for $C_{46}H_{56}I_4N_{10}NiO_4S_4Te_2$, C, 31.3; H, 3.2; N, 7.9%. Found: C, 31.3; H, 3.2; N, 8.0%. IR (KBr, cm^{-1}): 2971 (w), 1712 (s), 1680 (s), 1541 (s), 1454 (s, br), 1370 (m), 1285 (m), 1231 (m, br), 1122 (m), 1100 (m), 1074 (m), 1000 (w), 839 (w), 737 (m), 681 (m), 455 (w). MS ES (m/z): 1051.1387 (M^+) (calc. 1051.1393).

[Ni(PhTe-μ-I-TePh)$_2$(L^{Et})$_2$] (***6***): $(PhTe)_2$ (208 mg, 0.5 mmol) was dissolved in 5 mL MeOH and cooled to 0 °C. Upon cooling in an ice bath, I_2 (128 mg, 0.5 mmol) was added under permanent stirring. After 30 min, the ice bath was removed and the stirring was continued for one additional hour at room temperature. H_2L^{Et} (200 mg, 0.5 mmol) dissolved in 5 mL MeOH was added and the mixture was stirred at 45 °C for 10 minutes. $Ni(CH_3COO)_2 \cdot 4\ H_2O$ (63 mg, 0.25 mmol) in 1 mL MeOH was added to the resulting yellow solution. An orange-red solid quickly precipitated. After stirring at room temperature for 1 h, the product was filtered off, washed with cold MeOH and recrystallized from CH_2Cl_2/MeCN (9/1 v/v) to obtain orange-red crystals. Yield 419 mg (87%). Elemental analysis: Calcd. for $C_{58}H_{66}I_2N_{10}NiO_4S_4Te_4$, C, 37.6; H, 4.0; N, 7.1%. Found: C, 37.4; H, 3.9; N, 7.1%. IR (KBr, cm^{-1}): 2977 (w), 2932 (w), 1636 (s), 1549 (s, br), 1433(s), 1355 (m), 1313 (m), 1251 (w), 1209 (w), 1096 (m), 1074 (m), 998 (w), 840 (w), 736 (m), 690 (w), 455 (w).

Computational Studies

DFT calculations were performed on the high-performance computing systems of the Freie Universität Berlin ZEDAT (Curta) using the program package GAUSSIAN 16.[73,74] The gas phase geometry optimizations were performed using coordinates derived from the X-ray crystal structures using GAUSSVIEW.[74] The calculations were performed with the hybrid density functional B3LYP.[76–79] The triple-ζ relativistic pseudopotential def2-TZVPD basis set was applied to all atoms including the respective effective core potential (ECP) for Te.[79–81] All basis sets as well as the ECPs were obtained from the basis set exchange database.[82] Frequency calculations after the optimizations confirmed the convergence and no imaginary frequencies were obtained. Further analyses of the obtained wave-functions were performed with the free multifunctional wavefunction analyzer Multiwfn.[83] The reduced density gradient (RDG) method was used as implemented in Multiwfn and visualized using the VMD package.[84,85] Molecular orbitals were localized and analyzed using the NBO 6.0 routine es implemented in GAUSSIAN 16.[86] Criteria for the evaluation of hydrogen bonding are described in previous work,[86,87] while general descriptors and criteria for the evaluation of topological analyses of non-covalent interactions are described in standard references.[88–92] Chalcogen bonds have been identified in compounds **1**, **2** and **3** based on the localized orbital locator (LOL),[93] and their strength was assessed from the solid-state data according to reference.[94]

Frequency calculations after the optimization confirmed the convergence of the obtained geometry, which resembles the experimentally determined solid-state structure.

Supporting Information Summary

Supporting information containing more crystallographic details, spectroscopic data and more details about the computational studies is provided.

Acknowledgements

This work was gratefully supported by the German Academic Exchange Service (DAAD, Germany), by the Conselho Nacional de Desenvolvimento Científico e Tecnológico (CNPq. Brazil) with research scholarships for SSS (Processes 140349/2007-3 and 290017/2009-2), and by Coordenação de Aperfeiçoamento de Pessoal de Nível Superior (CAPES. Brazil), via the CAPES/PrInt initiative (88881.310412/2018-01). We gratefully acknowledge the assistance of the Core Facility BioSupraMol supported by the DFG and High-Performance-Computing (HPC) Centre of the Zentraleinrichtung für Datenverarbeitung (ZEDAT) of the Freie Universität Berlin for computational time and support. Special thanks go to Fabrício Bublitz (UFSM) for recording various NMR spectra. PTC and HHN acknowledge financial support from Vietnam National Foundation for Science and Technology Development (NAFOSTED) under Grant 104.03-2020.25. Open Access funding enabled and organized by Projekt DEAL.

Conflict of Interests

The authors declare no conflict of interest.

Data Availability Statement

The data that support the findings of this study are available in the supplementary material of this article.

Keywords: Tellurium · Transition metals · Self-assembly · Aroylthioureas · Density functional calculations

[1] F. A. Devillanova, W.-H. du Mont, *Handbook of Chalcogen Chemistry: New Perspectives in Sulfur, Selenium and Tellurium*, RSC Publishing, Cambridge **2013**.
[2] V. Lippolis, C. Santi, E. Leonardo, A. L. Braga, *Chalcogen Chemistry: Fundamentals and Applications*, RSC Publishing, London **2023**.
[3] A. Nordheider, J. D. Woollins, T. Chivers, *Chem. Rev.* **2015**, *115*, 10378.
[4] T. Chivers, R. S. Laitinen, *Chem. Soc. Rev.* **2015**, *44*, 1725.
[5] R. G. Pearson, *J. Am. Chem. Soc.* **1963**, *85*, 3533.
[6] B. Krebs, F.-P. Ahlers, *Adv. Inorg. Chem.* **1990**, *35*, 235.
[7] W. Levason, G. Reid, M. Victor, W. Zhang, *Polyhedron* **2009**, *28*, 4010.
[8] C. J. Carmalt, N. C. Norman, L. J. Farrugia, *Polyhedron* **1995**, *14*, 1405.
[9] E. S. Lang, G. N. Ledesma, U. Abram, M. Vega-Teijido, I. Caracelli, J. Zukerman-Schpector, *Z. Kristallogr.* **2006**, *221*, 166.
[10] G. A. Casagrande, E. S. Lang, B. Tirloni, R. A. Burrow, G. M. de Oliveira, S. S. Lemos, *Z. Anorg. Allg. Chem.* **2006**, *632*, 893.
[11] M. D. Rudd, D. L. Pahl, C. J. Hofkens, R. P. Feazell, *Phosphorus Sulfur Silicon Relat. Elem.* **2006**, *181*, 2023.
[12] E. S. Lang, G. A. Casagrande, G. M. de Oliveira, G. N. Ledesma, S. S. Lemos, E. E. Castellano, U. Abram, *Eur. J. Inorg. Chem.* **2006**, 958.
[13] D. L. Williams, V. L. H. Bevilacqua, P. A. Morson, W. T. Pennington, G. L. Schimek, N. T. Kawai, *Inorg. Chim. Acta* **2000**, *308*, 129.
[14] S. Husebye, K. W. Tornroos, *Acta Crystallogr. Sect. C.* **2000**, *56*, 1242.
[15] G. C. Rout, M. Seshasayee, G. Aravamudan, S. Sowrirajan, *Acta Crystallogr. Sect. C* **1984**, *40*, 963.
[16] C. Gurnani, M. Jura, W. Levason, R. Ratnani, G. Reid, M. Webster, *Dalton Trans.* **2009**, 4122.
[17] Cambridge Crystallographic Database, version 5.44, April 2023; C. R. Groom, I. J. Bruno, M. P. Lightfoot, S. C. Ward, *Acta Cryst.* **2016**, *B72*, 171–179.
[18] K. von Deuten, W. Schnabel, G. Klar, *Cryst. Struct. Commun.* **1980**, *9*, 161.
[19] J. E. Drake, L. M. Khasrou, A. G. Mislankar, R. Ratnani, *Can. J. Chem.* **1999**, *77*, 1262.
[20] L. Beyer, E. Hoyer, J. Liebscher, H. Hartmann, *Z. Chem.* **1981**, *21*, 81.
[21] K. R. Koch, *Coord. Chem. Rev.* **2001**, *216–217*, 473.
[22] Z. Weigun, Y. Wen, Q. Lihua, Z. Yong, Y. Zhengfeng, *J. Mol. Struct.* **2005**, *749*, 89.
[23] M. Kampf, R. Richter, S. Gerber, R. Kirmse, *Z. Anorg. Allg. Chem.* **2004**, *630*, 1437.
[24] H. H. Nguyen, U. Abram, *Inorg. Chem.* **2007**, *46*, 5310.
[25] N. Gunasekaran, S. W. Ng, E. R. T. Tiekink, R. Karvembu, *Polyhedron* **2012**, *34*, 41.
[26] U. Braun, R. Richter, J. Sieler, A. I. Yanovsky, Y. T. Struchkov, *Z. Anorg. Allg. Chem.* **1985**, *529*, 201.
[27] S.-Y. Wu, X.-Y. Zhao, H.-P. Li, Y. Yang, H. W. Roesky, *Z. Anorg. Allg. Chem.* **2015**, *641*, 883.
[28] W. Bensch, M. Z. Schuster, *Z. Anorg. Allg. Chem.* **1992**, *611*, 99.
[29] D.-J. Che, G. Li, X.-L. Yao, Y.-Z., D.-P. Zhou, *J. Chem. Soc. Dalton Trans.* **1999**, 2683.
[30] N. Gunasekaran, P. Ramesh, M. N. G. Ponnuswamy, R. Karvembu, *Dalton Trans.* **2011**, *40*, 12519.
[31] B. Schmitt, T. I. A. Gerber, E. Hosten, R. Betz, *Inorg. Chem. Commun.* **2012**, *24*, 136.
[32] Y.-M. Zhang, H.-X. Pang, C. Cao, T.-B. Wei, *J. Coord. Chem.* **2008**, *61*, 1663.
[33] N. Selvakumaran, L. Sandhiya, N. S. P. Bhuvanesh, K. Senthilkumar, R. Karvembu, *New J. Chem.* **2016**, *40*, 5401.
[34] G. L. Tember, A. S. R. Murty, *Curr. Sci.* **1983**, *52*, 1013.
[35] U. Schröder, L. Beyer, J. Sieler, *Inorg. Chem. Commun.* **2000**, *3*, 630.
[36] C. N. Noufele, C. T. Pham, A. Hagenbach, U. Abram, *Inorg. Chem.* **2018**, *57*, 12255.
[37] C. T. Pham, M. R. Jungfer, U. Abram, *New. J. Chem.* **2020**, *44*, 3672.
[38] H. H. Nguyen, U. Abram, C. T. Pham, *Vietnam. J. Chem. Int. Ed.* **2022**, *60*, 622.
[39] C. T. Pham, T. H. Nguyen, K. Matsumoto, H. H. Nguyen, *Eur. J. Inorg. Chem.* **2019**, 4142.
[40] M. I. de Oliveira, G. P. Chuy, B. S. Vizzotto, R. A. Burrow, E. S. Lang, S. S. dos Santos, *Inorg. Chim. Acta* **2020**, *512*, 119871.
[41] H. H. Nguyen, J. J. Jegathesh, A. Takiden, D. Hauenstein, C. T. Pham, C. D. Le, U. Abram, *Dalton Trans.* **2016**, *45*, 10771.
[42] S. F. Sucena, T. I. Demirer, A. Baitullina, A. Hagenbach, J. Grewe, S. Spreckelmeyer, J. März, A. Barkleit, P. I. da Silva Maia, H. H. Nguyen, U. Abram, *Molecules* **2023**, *28*, 5421.
[43] S. F. Sucena, T. T. Pham, A. Hagenbach, C. T. Pham, U. Abram, *Eur. J. Inorg. Chem.* **2020**, 4341.
[44] A. Baitullina, G. Claude, S. F. Sucena, E. Nisli, C. Scholz, P. Bhardwaj, H. Amthauer, W. Brenner, C. Geppert, C. Gorges, U. Abram, P. I. da Silva Maia, S. Spreckelmeyer, *EJNMMI Radiopharm. Chem.* **2023**, *8*, 40.
[45] K. R. Koch, S. Bourne, *J. Mol. Struct.* **1998**, *441*, 11.
[46] H. H. Nguyen, J. J. Jegathesh, P. I. da Silva Maia, V. M. Deflon, R. Gust, S. Bergemann, U. Abram, *Inorg. Chem.* **2009**, *48*, 9356.
[47] A. A. Casagrande, E. Schulz Lang, B. Tirloni, R. A. Burrow, G. M. de Oliveira, S. S. Lemos, *Z. Anorg. Allg. Chem.* **2006**, *632*, 893.
[48] S. Behrendt, L. Beyer, F. Dietze, E. Kleinpeter, E. Hoyer, *Inorg. Chim. Acta* **1980**, *43*, 141.
[49] S. Saito, J. Zhang, K. Tanida, S. Takahashi, T. Koizumi, *Tetrahedron* **1999**, *55*, 2545.
[50] W.-W. du Mont, H.-J. Kroth, *Z. Naturforsch.* **1981**, *36b*, 332.
[51] H. Schumann, M. Magerstädt, *Inorg. Chem. Comm.* **2008**, *11*, 1478.
[52] H. H. Nguyen, U. Abram, *Inorg. Chem. Commun.* **2008**, *11*, 1478.
[53] T. J. Egan, K. R. Koch, P. L. Swan, C. Clarkson, D. A. van Schalkwyk, P. J. Smith, *J. Med. Chem.* **2004**, *47*, 2926.
[54] S. S. dos Santos, E. S. Lang, G. M. de Oliveira, *J. Organomet. Chem.* **2007**, *692*, 3081.
[55] G. M. de Oliveira, G. A. Casagrande, E. S. Lang, R. M. Muzzi, S. S. Lemos, *J. Organomet. Chem.* **2009**, *694*, 2463.
[56] E. S. Lang, G. M. de Oliveira, R. M. Fernandes Jr., E. M. Vazquez-Lopez, *Inorg. Chem. Commun.* **2003**, *6*, 869.
[57] E. S. Lang, G. M. de Oliveira, G. N. Ledesma, *Z. Anorg. Allg. Chem.* **2005**, *631*, 1524.
[58] A. J. Z. Londero, N. R. Pineda, V. Matos, P. C. Piquini, U. Abram, E. S. Lang, *J. Organomet. Chem.* **2020**, *929*, 121553.
[59] E. S. Lang, G. M. de Oliveira, G. A. Casagrande, *J. Organomet. Chem.* **2006**, *691*, 59.
[60] S. S. dos Santos, E. S. Lang, R. A. Burrow, *J. Braz. Chem. Soc.* **2006**, *17*, 1566.
[61] E. Schulz Lang, R. M. Fernandes Jr., E. T. Silveira, U. Abram, E. M. Vazquez-Lopez, *Z. Anorg. Allg. Chem.* **1999**, *625*, 1401.
[62] K. J. Irgolic, in *Synthetic Methods of Organometallic and Inorganic Chemistry (Herrmann/Brauer)*(Eds: W. A. Herrmann, C. Zybill), Vol. 4, Georg Thieme Verlag, Stuttgart, Germany **1997**, 184.
[63] N. W. Alcock, W. D. Harrison, *Acta Cryst.* **1982**, *B38*, 2677.
[64] N. W. Alcock, W. D. Harrison, *J. Chem. Soc. Dalton Trans.* **1984**, 869.
[65] G. M. Sheldrick, *SADABS*, University of Göttingen, Göttingen, Germany **2014**.
[66] P. Coppens, *The Evaluation of Absorption and Extinction in Single-Crystal Structure Analysis*, CrystallographicComputing, Muksgaard, Copenhagen **1979**.
[67] G. M. Sheldrick, *Acta Crystallogr. Sect. A* **2008**, *64*, 112.
[68] G. M. Sheldrick, *Acta Crystallogr. Sect. C: Struct. Chem.* **2015**, *71*, 3.
[69] L. J. Farrugia, *J. Appl. Cryst.* **2012**, *45*, 849.
[70] O. V. Dolomanov, L. J. Bourhis, R. J. Gildea, J. A. Howard, H. Puschmann, *J. Appl. Crystallogr.* **2009**, *42*, 339.
[71] Diamond - Crystal and Molecular Structure Visualization, vers. 4.0. Crystal Impact, Dr. H. Putz & Dr. K. Brandenburg GbR: Bonn, Germany **2023**.
[72] Deposition numbers CCDC-2322091 (for **1**), CCDC-2322092 (for **2**), CCDC-2322093 (for **3**), CCDC-2322094 (for **4**), CCDC-2322095 (for **5e**) and CCDC-2322096 (for **6**) contain the supplementary crystallographic data for this paper. These data are provided free of charge by the joint Cambridge Crystallographic Data Centre and Fachinformationszentrum Karlsruhe Access Structures service.

[73] High performance computing (HPC) system Curta at Freie Universität Berlin, DOI: 10.17169/refubium-26754.
[74] M. J. Frisch, G. W. Trucks, H. B. Schlegel, G. E. Scuseria, M. A. Robb, J. R. Cheeseman, G. Scalmani, V. Barone, G. A. Petersson, H. Nakatsuji, X. Li, M. Caricato, A. V. Marenich, A. J. Bloino, B. G. Janesko, R. Gomperts, B. Mennucci, H. P. Hratchian, J. V. Ortiz, A. F. Izmaylov, J. L. Sonnenberg, D. Williams-Young, F. Ding, F. Lipparini, F. Egidi, J. Goings, B. Peng, A. Petrone, T. Henderson, D. Ranasinghe, V. G. Zakrzewski, J. Gao, N. Rega, G. Zheng, W. Liang, M. Hada, M. Ehara, K. Toyota, R. Fukuda, J. Hasegawa, M. Ishida, T. Nakajima, Y. Honda, O. Kitao, H. Nakai, T. Vreven, K. Throssell, J. A. Montgomery Jr., J. E. Peralta, F. Ogliaro, M. J. Bearpark, J. J. Heyd, E. N. Brothers, K. N. Kudin, V. N. Staroverov, T. A. Keith, R. Kobayashi, J. Normand, K. Raghavachari, A. P. Rendell, J. C. Burant, S. S. Iyengar, J. Tomasi, M. Cossi, J. M. Millam, M. Klene, C. Adamo, R. Cammi, J. W. Ochterski, R. L. Martin, K. Morokuma, O Farkas, J. B. Foresman, D. J. Fox, Gaussian 16, Revision A.02, Gaussian, Inc., Wallingford CT **2016**.
[75] R. Dennington, T. A. Keith, J. M. Millam, GaussView, Version 6, Semichem Inc., Shawnee Mission, KS **2016**.
[76] S. H. Vosko, L. Wilk, M. Nusair, *Can. J. Phys.* **1980**, *58*, 1200.
[77] A. D. Becke, *J. Chem. Phys.* **1993**, *98*, 5648.
[78] C. Lee, W. Yang, R. G. Parr, *Phys. Rev.* **1988**, *B37*, 785.
[79] K. A. Peterson, D. Figgen, E. Goll, H. Stoll, M. Dolg, *J. Chem. Phys.* **2003**, *119*, 11113.
[80] D. Rappoport, F. Furche, *J. Chem. Phys.* **2010**, *133*, 134105.
[81] F. Weigend, R. Ahlrichs, *Phys. Chem. Chem. Phys.* **2005**, *7*, 3297.
[82] K. L. Schuchardt, B. T. Didier, T. Elsethagen, L. Sun, V. Gurumoorthi, J. Chase, J. Li, T. L. Windus, *J. Chem. Inf. Model.* **2007**, *47*, 1045.
[83] T. Lu, F. Chen, *J. Comput. Chem.* **2012**, *33*, 580.
[84] E. R. Johnson, S. Keinan, P. Mori-Sánchez, J. Contreras-García, A. J. Cohen, W. Yang, *J. Am. Chem. Soc.* **2010**, *132*, 6498.
[85] W. Humphrey, A. Dalke, K. Schulten, *J. Molec. Graphics* **1996**, *14*, 33.
[86] E. D. Glendening, C. R. Landis, F. Weinhold, *J. Comput. Chem.* **2013**, *34*, 1429.
[87] C. Tantardini, *J. Comput. Chem.* **2019**, *40*, 937.
[88] S. J. Grabowski *J. Phys. Org. Chem.* **2004**, *17*, 18.
[89] R. F. W. Bader, *Atoms in Molecules: A Quantum Theory*, Clarendon, Oxford, U. K. **1990**.
[90] R. Hilal, S. G. Aziz, A. O. Alyoubi, S. Elroby, *Procedia Comput. Sci.* **2015**, *51*, 1872.
[91] W. Wang, B. Ji, Y. Zhang, *J. Phys. Chem. A* **2009**, *113*, 8132.
[92] C. S. López, A. R. de Lera, *Curr. Org. Chem.* **2011**, *15*, 3576.
[93] V. Matos, A. J. Z. Londero, M. Roca Jungfer, U. Abram, E. S. Lang, *Eur. J. Inorg. Chem.* **2023**, *26*, e202300478.
[94] M. C. Aragoni, M. Arca, V. Lippolis, A. Pintus, Y. Torubaev, E. Podda, *Molecules* **2023**, *28*, 3133.

Manuscript received: June 17, 2024
Revised manuscript received: July 2, 2024
Accepted manuscript online: July 8, 2024
Version of record online: August 25, 2024